

University of Nebraska - Lincoln

DigitalCommons@University of Nebraska - Lincoln

Final Reports & Technical Briefs from Mid-America
Transportation Center

Mid-America Transportation Center

2010

Impact of Truck Loading on Design and Analysis of Asphaltic Pavement Structures

Yong-Rak Kim

University of Nebraska-Lincoln, yong-rak.kim@unl.edu

Hokie Ban

University of Nebraska-Lincoln

Soohyok Im

University of Nebraska-Lincoln

Follow this and additional works at: <https://digitalcommons.unl.edu/matreports>



Part of the [Civil Engineering Commons](#)

Kim, Yong-Rak; Ban, Hokie; and Im, Soohyok, "Impact of Truck Loading on Design and Analysis of Asphaltic Pavement Structures" (2010). *Final Reports & Technical Briefs from Mid-America Transportation Center*. 23.

<https://digitalcommons.unl.edu/matreports/23>

This Article is brought to you for free and open access by the Mid-America Transportation Center at DigitalCommons@University of Nebraska - Lincoln. It has been accepted for inclusion in Final Reports & Technical Briefs from Mid-America Transportation Center by an authorized administrator of DigitalCommons@University of Nebraska - Lincoln.



MID-AMERICA TRANSPORTATION CENTER

Report # MATC-UNL: 223

Final Report



Impact of Truck Loading on Design and Analysis of Asphaltic Pavement Structures

Yong-Rak Kim, Ph.D.

Assistant Professor

Department of Civil Engineering

University of Nebraska-Lincoln

Hoki Ban, Ph.D.

Soohyok Im, Ph.D. student



2010

A Cooperative Research Project sponsored by the
U.S. Department of Transportation Research and
Innovative Technology Administration

The contents of this report reflect the views of the authors, who are responsible for the facts and the accuracy of the information presented herein. This document is disseminated under the sponsorship of the Department of Transportation University Transportation Centers Program, in the interest of information exchange.
The U.S. Government assumes no liability for the contents or use thereof.

MATC

Impact of Truck Loading on Design and Analysis of Asphaltic Pavement Structures

Yong-Rak Kim, Ph.D.
Assistant Professor
Department of Civil Engineering-UNL

Hoki Ban
Post-Doctoral Research Associate
Department of Civil Engineering-UNL

Soohyok Im
Ph.D. student
Department of Civil Engineering-UNL

A Report on Research Sponsored By

Mid-America Transportation Center
University of Nebraska-Lincoln

December 2009

Technical Report Documentation Page

1. Report No. 25-1121-0001-223	2.	3. Recipient's Accession No.	
4. Title and Subtitle Impact of Truck Loading on Design and Analysis of Asphaltic Pavement Structures		5. Report Date December 2009	
		6.	
7. Author(s) Yong-Rak Kim, Hoki Ban, and Soohyok Im.		8. Performing Organization Report No. 25-1121-0001-223	
9. Performing Organization Name and Address		10. Project/Task/Work Unit No.	
		11. Contract © or Grant (G) No.	
12. Sponsoring Organization Name and Address Mid-America Transportation Center U.S. Department of Transportation Region VII University Transportation Center University of Nebraska-Lincoln 2200 Vine Street P.O. Box 830851 Lincoln, Nebraska 68583-0851		13. Type of Report and Period Covered	
		14. Sponsoring Agency Code MATC TRB RiP No. 18466	
15. Supplementary Notes			
16. Abstract (Limit: 200 words) Mechanistic-Empirical Pavement Design Guide (MEPDG) is an improved methodology for pavement design and the evaluation of paving materials. However, in spite of significant advancements to pre-existing traditional design methods, the MEPDG is known to be limited in its accurate prediction of mechanical responses and damage in asphaltic pavements. This restriction is both due to the use of simplified structural analysis methods, and a general lack of understanding of the fundamental constitutive behavior and damage mechanisms in paving materials. This is additionally affected by the use of circular tire loading configurations. Performance prediction and pavement life are determined based on the simple layered elastic theory and the empirically-developed failure criteria: the so-called transfer functions. To model pavement performance in a more appropriate manner, this study attempts finite element modeling to account for viscoelastic paving materials. Mechanical responses between the finite element simulations and the MEPDG analyses are compared to monitor any significant differences that are relevant to better pavement analysis and design. Pavement performance and the corresponding design life between the two approaches are further compared and discussed.			
17. Document Analysis/Descriptors		18. Availability Statement	
19. Security Class (this report)	20. Security Class (this page)	21. No. of Pages 47	22. Price

Table of Contents

Acknowledgments	vi
Executive Summary	vii
Chapter 1 Introduction	1
1.1 Research Objectives and Scope	2
1.2 Organization of the Report	3
Chapter 2: Literature Review	4
2.1 MEPDG Analysis	4
2.2 MEPDG Inputs	5
2.2.1 Climatic Inputs	7
2.2.2 Traffic Inputs	8
2.2.3 Material Inputs	8
2.3 Pavement Distresses Considered	11
2.3.1 Rutting in the MEPDG	11
2.4 Finite Element Analysis for Flexible Pavements	13
2.4.1 Axisymmetric Approach	15
2.4.2 Two Dimensional (2-D) Plane Strain Approach	16
2.4.3 Three dimensional (3-D) Approach	17
2.5 Material Models for Finite Element Analysis	18
Chapter 3 MEPDG Analysis	20
Chapter 4 Finite Element Analysis	23
4.1 Preliminary Analyses	24
4.2 Finite Element Modeling of the Pavement Structure	36
Chapter 5 Analysis Results and Discussion	39
Chapter 6 Summary and Conclusions	43
References	45

List of Figures

Figure 2.1 MEPDG Design Procedure (NCHRP 1-37A, 2004).....	5
Figure 2.2 Three Typical FE Analysis Models for Pavements.....	14
Figure 2.3 Generalized Maxwell Model.....	19
Figure 3.1 A Typical Class 9 Truck.....	21
Figure 3.2 Pavement Structures for this Study and Material Properties for the MEPDG.....	22
Figure 4.1 Four Different Sizes of FE Domain Analyzed to Investigate End Effects.....	25
Figure 4.2 Surface Displacements vs. Thickness of the Sub-grade Layer.....	26
Figure 4.3 Finite Element Meshes with Infinite Elements.....	28
Figure 4.4 A Typical Single Truck Axle with Dual Tires.....	31
Figure 4.5 Finite Element Meshes and Boundary Conditions of Each Modeling.....	33
Figure 4.6 Axisymmetric Dimension of the Finite Element Mesh for this Study.....	36
Figure 4.7 Loading Configuration of the Class 9 Truck Used for the FE Modeling.....	37
Figure 5.1 Vertical Displacement vs. Time (from FEM).....	40
Figure 5.2 Rut Depth vs. Time and Its Extrapolation (from FEM).....	40
Figure 5.3 Comparison of Pavement Performance and Life between MEPDG and FEM.....	41

List of Tables

Table 2.1 Major Material Types for the MEPDG (AASHTO, 2008).....	9
Table 2.2 Asphalt Materials and the Test Protocols to Measure Material Properties for New and Existing HMA Layers (AASHTO, 2008).....	10
Table 2.3 Summary of FE Modeling Approaches (Yoo, 2007).....	14
Table 3.1 Summary of Traffic and Climate Inputs for MEPDG Analysis.....	20
Table 4.1 FE Simulation Results with Different Number of Elements vs. JULEA Results.....	27
Table 4.2 Comparison of Computation Costs of Each Model.....	29
Table 4.3 Summary of FE Simulations and Comparison with JULEA.....	30
Table 4.4 Summary of Pavement Responses at Various Locations Resulting from Three Different Modeling Approaches.....	35
Table 4.5 Mechanical Material Properties of Each Layer for the FE Modeling.....	38

Acknowledgments

The authors would like to thank the Mid-America Transportation Center (MATC) for their financial support needed to complete this study.

Executive Summary

Mechanistic-Empirical Pavement Design Guide (MEPDG) is an improved methodology for pavement design and the evaluation of paving materials. However, in spite of significant advancements to pre-existing traditional design methods, the MEPDG is known to be limited in its accurate prediction of mechanical responses and damage in asphaltic pavements. This restriction is both due to the use of simplified structural analysis methods, and a general lack of understanding of the fundamental constitutive behavior and damage mechanisms in paving materials. This is additionally affected by the use of circular tire loading configurations. Performance prediction and pavement life are determined based on the simple layered elastic theory and the empirically-developed failure criteria: the so-called transfer functions. To model pavement performance in a more appropriate manner, this study attempts finite element modeling to account for viscoelastic paving materials. Mechanical responses between the finite element simulations and the MEPDG analyses are compared to monitor any significant differences that are relevant to better pavement analysis and design. Pavement performance and the corresponding design life between the two approaches are further compared and discussed.

Chapter 1 Introduction

A new Mechanistic-Empirical Pavement Design Guide (MEPDG) has recently been developed (NCHRP 1-37A 2004) and is currently under validation-implementation by many states. The design guide represents a challenging innovation in the way pavement design and analysis is performed. Design inputs include traffic (various axle configurations with their detail distributions), material characterization, climatic factors, performance criteria, and other factors. However, in spite of significant advancements, the MEPDG is known to be limited in its ability to accurately predict mechanical responses in asphaltic pavements. This is due to the use of simplified structural analysis methods, a general lack of understanding of the fundamental constitutive behavior and damage mechanisms in paving materials, and the use of circular tire loading configurations. Performance prediction and pavement life are determined based on the simple layered elastic theory and the empirically-developed failure criteria: the so-called transfer functions.

The multi-layered elastic theory has been widely used for the structural analysis of flexible pavements. Nevertheless, it has been observed that results from layered elastic analyses do not correlate well with field measurements. The mismatch between analysis results and field measurements can be attributed to many factors. One of the primary factors is strongly related to the elastic assumption, which is not suitable to characterize the time-rate-temperature dependent response of an asphalt layer in pavements. Improving a designer's ability to understand pavement mechanics and to predict pavement performance and life will greatly improve pavement structural designs. A

mechanistic approach can be pursued with a more realistic characterization of paving materials, pavement structures, and truck load simulations. Even if it may not be immediately practical, the mechanistic approach can provide significant insights into the empirical weakness of the MEPDG.

To this end, this study investigates pavement performance predictions from both the MEPDG approach and the mechanistic approach based on the finite element method (FEM). For mechanistic analysis using the FEM, the pavement is modeled in an axisymmetric structure with a viscoelastic asphalt layer. Since axisymmetric analysis is only capable of simulating a single circular loading, the superposition principle was employed to account for multiple tire configurations. Mechanical responses between the finite element simulations and the MEPDG analyses are compared to monitor any significant differences. Pavement performance and the design life between the two approaches are compared and discussed.

1.1 Research Objectives and Scope

The primary objective of this study is to investigate pavement performance predictions from both the MEPDG approach and the mechanistic approach based on the FEM. Performance and life of pavements is a function of several parameters such as layer thickness, lane width, contact area of the tire, pressure distribution, applied load, loading frequency, tire configurations, material properties, and failure criteria. Energy dissipation due to several effects, such as viscoelasticity, crack-associated damage, aging of materials, and environmental effects should be included to accurately predict the long-term behavior of asphalt pavements. However, as a first step of this research, this study investigates the effects of only one design parameter. The properties of a hot-mix asphalt,

HMA, surface layer on pavement performance and life will be predicted by rutting, which will serve as the only type of failure mode for this experiment. Other design variables and pavement failure modes such as cracking are not considered in this study. Furthermore, this study does not include all environmental conditions at this time. The current goal is a mechanistic model with the least number of empirical variables and assumptions. This model will be compared with the MEPDG approach, which predicts long-term pavement service life based on empirically developed transfer functions.

1.2 Organization of the Report

This report is composed of six chapters. Following this introduction, Chapter 2 summarizes the literature review on MEPDG analysis procedures and finite element, FE, analysis. Chapter 3 presents MEPDG analysis including its pavement structure and required inputs. FE analysis is described in Chapter 4 as a parallel to the MEPDG analysis method. Chapter 5 presents analysis results and discussion. Finally, Chapter 6 provides a summary and conclusions for this study.

Chapter 2: Literature Review

Many researchers have engaged in tremendous efforts to develop design tools for flexible pavements. Among those, the MEPDG and FE analyses are most commonly used to perform pavement design and analysis. In this chapter, the background of the MEPDG with general procedures and FE studies for flexible pavement analysis are described.

2.1 MEPDG Analysis

The MEPDG is an analysis tool which enables prediction of pavement performances over time for a given pavement structure subjected to variable conditions, such as traffic and climate. The mechanistic-empirical design of new and reconstructed flexible pavements requires an iterative hands-on approach by the designer. The designer must select a trial design and then analyze the design to determine if it meets the performance criteria established by the designer. If the trial design does not satisfy the performance criteria, the design is modified and reanalyzed until the design satisfies the performance criteria (NCHRP 1-37A 2004).

The procedure of the MEPDG depends heavily on the characterization of the fundamental engineering properties of paving materials. It requires a number of input data in four major categories: traffic, material characterization and properties, environmental influences, and pavement response and distress models. As shown in figure 2.1, the design procedure accounts for the environmental conditions that may affect pavement response. These pavement responses are determined by mechanistic procedures. The mechanistic method determines structural response, or strain and stress, in the pavement structure. The transfer function is utilized to directly calculate individual

distresses--top-down cracking, bottom-up cracking, transverse cracking, and rutting--in an empirical manner.

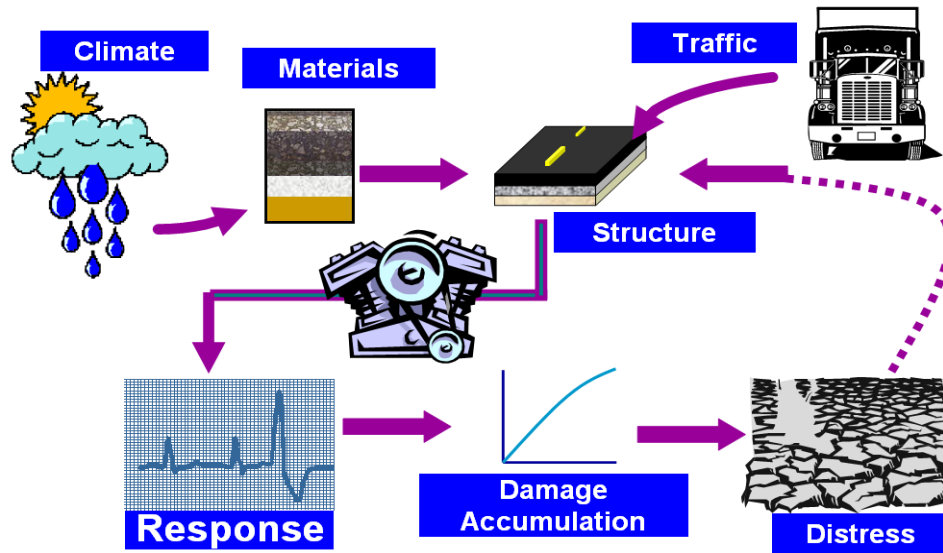


Fig. 2.1 MEPDG Design Procedure (NCHRP 1-37A 2004)

2.2 MEPDG Inputs

The MEPDG represents a challenging innovation in the way pavement design is performed; design inputs include traffic (full load spectra for various axle configurations), material and sub-grade characterization, climatic factors, performance criteria, and many other factors. One of the most interesting aspects of the design procedure is its hierarchical approach: that is, the consideration of different levels of inputs. Level 1 requires the engineer to obtain the most accurate design inputs (e.g., direct testing of materials, on-site traffic load data, etc.). Level 2 requires testing, but the use of correlations is allowed (e.g., sub-grade modulus estimated through correlation with another test). Level 3 generally uses estimated values. Thus, Level 1 has the least

possible error associated with inputs, Level 2 uses regional defaults or correlations, and Level 3 is based on the default values. This hierarchical approach enables the designer to select the design input depending on the degree of significance of the project and availability of resources. The three levels of inputs are described as follows (NCHRP 1-37A 2004):

- Level 1 input provides the highest level of accuracy and, accordingly, would have the lowest level of uncertainty or error. Level 1 design generally requires project-specific input such as material input measured by laboratory or field testing, site-specific axle load spectra data, or nondestructive deflection testing. Because such inputs require additional time and resources to obtain, Level 1 inputs are generally used for research, forensic studies, or projects in which a low probability of failure is important.
- Level 2 input supplies an intermediate level of accuracy that is closest to the typical procedures used with earlier editions of the AASHTO guide. Level 2 input would most likely be user-selected from an agency database, derived from a limited testing program, or be estimated through correlations. Examples of input includes estimating asphalt concrete dynamic modulus from binder, aggregate, and mix properties; estimating Portland cement concrete elastic moduli from compressive strength tests; or using site-specific traffic volume and traffic classification data in conjunction with agency-specific axle load spectra. Level 2 input is most applicable for routine projects with no special degree of significance.

- Level 3 input affords the lowest level of accuracy. This level might be used for designs where there are minimal consequences of early failure, as with lower volume roads. Inputs typically would be user-selected values or typical averages for the region. Examples include default unbound materials, resilient modulus values, or the default Portland cement concrete coefficient of thermal expansion for a given mix classes, and aggregates used by an agency.

2.2.1 Climatic Inputs

In the 1993 AASHTO design guide, the climatic variables were handled with seasonal adjustments and application of drainage coefficients. In the MEPDG, however, temperature changes and moisture profiles in the pavement structure and sub-grade over the design life of a pavement are fully considered by using a sophisticated climatic modeling tool called the Enhanced Integrated Climatic Model (EICM). The EICM model simulates changes in behavior and characteristics of pavement and sub-grade materials in conjunction with climatic conditions over the design life of the pavement. To use this model, a relatively large number of input parameters are needed and include the following (NCHRP 1-37A 2004):

- General information
- Weather-related information
- Groundwater table depth
- Drainage and surface properties, and
- Pavement structure materials.

2.2.2 Traffic Inputs

For traffic analysis, the inputs for the MEPDG are much more complicated than those required by the 1993 AASHTO design guide. In the 1993 design guide the primary traffic-related input was the total design 80 kN equivalent single axle loads, ESALs, expected over the design life of the pavement. In contrast, the more sophisticated traffic analysis in the MEPDG uses axle load spectra data. The following traffic related input is required for the MEPDG (NCHRP 1-37A 2004):

- Base year truck-traffic volume (the year used as the basis for design computation)
- Vehicle (truck) operational speed
- Truck-traffic directional and lane distribution factors
- Vehicle (truck) class distribution
- Axle load distribution factors
- Axle and wheel base configurations
- Tire characteristics and inflation pressure
- Truck lateral distribution factors, and
- Truck growth factors.

2.2.3 Material Inputs

There are a number of material inputs for the design procedure and various types of test protocols to measure material properties. Table 2.1 summarizes different types of materials involved in the MEPDG, and table 2.2 shows the material properties of the HMA layer and test protocols to characterize the HMA materials.

Table 2.1 Major Material Types for the MEPDG (AASHTO 2008)

<p><u>Asphalt Materials</u></p> <ul style="list-style-type: none"> • Stone Matrix Asphalt (SMA) • Hot Mix Asphalt (HMA) <ul style="list-style-type: none"> ○ Dense Graded ○ Open Graded Asphalt ○ Asphalt Stabilized Base Mixes ○ Sand Asphalt Mixtures • Cold Mix Asphalt <ul style="list-style-type: none"> ○ Central Plant Processed ○ In-Place Recycled <p><u>PCC Materials</u></p> <ul style="list-style-type: none"> • Intact Slabs – PCC <ul style="list-style-type: none"> ○ High Strength Mixes ○ Lean Concrete Mixes • Fractured Slabs <ul style="list-style-type: none"> ○ Crack/Seat ○ Break/Seat ○ Rubblized <p><u>Chemically Stabilized Materials</u></p> <ul style="list-style-type: none"> • Cement Stabilized Aggregate • Soil Cement • Lime Cement Fly Ash • Lime Fly Ash • Lime Stabilized Soils • Open graded Cement Stabilized Aggregate 	<p><u>Non-Stabilized Granular Base/Subbase</u></p> <ul style="list-style-type: none"> • Granular Base/Subbase • Sandy Subbase • Cold Recycled Asphalt (used as aggregate) <ul style="list-style-type: none"> ○ RAP (includes millings) ○ Pulverized In-Place • Cold Recycled Asphalt Pavement (HMA plus aggregate base/subbase) <p><u>Sub-grade Soils</u></p> <ul style="list-style-type: none"> • Gravelly Soils (A-1;A-2) • Sandy Soils <ul style="list-style-type: none"> ○ Loose Sands (A-3) ○ Dense Sands (A-3) ○ Silty Sands (A-2-4;A-2-5) ○ Clayey Sands (A-2-6; A-2-7) • Silty Soils (A-4;A-5) • Clayey Soils, Low Plasticity Clays (A-6) <ul style="list-style-type: none"> ○ Dry-Hard ○ Moist Stiff ○ Wet/Sat-Soft • Clayey Soils, High Plasticity Clays (A-7) <ul style="list-style-type: none"> ○ Dry-Hard ○ Moist Stiff ○ Wet/Sat-Soft <p><u>Bedrock</u></p> <ul style="list-style-type: none"> • Solid, Massive and Continuous • Highly Fractured, Weathered
---	---

Table 2.2 Asphalt Materials and the Test Protocols to Measure Material Properties for New and Existing HMA Layers (AASHTO 2008)

Design Type	Measured Property	Source of Data		Recommended Test Protocol and/or Data Source
		Test	Estimate	
New HMA (new pavement and overlay mixtures), as built properties prior to opening to truck traffic	Dynamic modulus	X		AASHTO TP 62
	Tensile strength	X		AASHTO T 322
	Creep Compliance	X		AASHTO T 322
	Poisson's ratio		X	National test protocol unavailable. Select MEPDG default relationship
	Surface shortwave absorptivity		X	National test protocol unavailable. Use MEPDG default value.
	Thermal conductivity	X		ASTM E 1952
	Heat capacity	X		ASTM D 2766
	Coefficient of thermal contraction		X	National test protocol unavailable. Use MEPDG default values.
	Effective asphalt content by volume	X		AASHTO T 308
	Air voids	X		AASHTO T 166
	Aggregate specific gravity	X		AASHTO T 84 and T 85
	Gradation	X		AASHTO T 27
	Unit Weight	X		AASHTO T 166
	Voids filled with asphalt (VFA)	X		AASHTO T 209
Existing HMA mixtures, in-place properties at time of pavement evaluation	FWD backcalculated layer modulus	X		AASHTO T 256 and ASTM D 5858
	Poisson's ratio		X	National test protocol unavailable. Use MEPDG default values.
	Unit Weight	X		AASHTO T 166 (cores)
	Asphalt content	X		AASHTO T 164 (cores)
	Gradation	X		AASHTO T 27 (cores or blocks)
	Air voids	X		AASHTO T 209 (cores)
	Asphalt recovery	X		AASHTO T 164/T 170/T 319 (cores)
Asphalt (new, overlay, and existing mixtures)	Asphalt Performance Grade (PG), OR	X		AASHTO T 315
	Asphalt binder complex shear modulus (G^*) and phase angle (δ), OR	X		AASHTO T 49
	Penetration, OR	X		AASHTO T 53
	Ring and Ball Softening Point			AASHTO T 202
	Absolute Viscosity	X		AASHTO T 201
	Kinematic Viscosity			AASHTO T 228
Specific Gravity, OR				
Brookfield Viscosity	X		AASHTO T 316	

Note: The global calibration factors included in version 1.0 of the MEPDG software for HMA pavements were determined using the NCHRP 1-37A viscosity based predictive model for dynamic modulus.

2.3 Pavement Distresses Considered

The MEPDG uses JULEA, a multilayer elastic analysis program, employed to determine the mechanical responses (i.e., stresses, strains, and displacements) in flexible pavement systems resulting from both traffic loads and climate factors (temperature and moisture). These responses are then incorporated with performance prediction models which accumulate monthly damage over the whole design period: the MEPDG analysis is based on the incremental damage approach.

The accumulated damage at any time is related to specific distresses – such as fatigue cracking (bottom-up and top-down), rutting, thermal cracking, and pavement roughness – all of which are predicted using field calibrated models. This is the primary empirical component of the mechanistic-empirical design procedure (NCHRP 1-37A 2004).

In this study, as previously mentioned, rutting is considered as the pavement failure criterion to compare the performance predictions of the MEPDG and FE analyses. A more detailed description of the rutting estimated by the MEPDG is provided herein. Theoretical details of other distress models--bottom-up cracking, top-down cracking, thermal cracking, and roughness--can be found in the guide (NCHRP 1-37A 2004).

2.3.1 Rutting in the MEPDG

Rutting is one of the primary distresses in flexible pavement systems. It is caused by the plastic or permanent deformation in the HMA, unbound layers, and foundation soils. The plastic deformation is computed by dividing each layer into a number of sub-layers, computing the plastic strain in each sub-layer, and adding the resulting plastic (permanent) deformation as expressed in the following equation:

$$PD = \sum_{i=1}^{NSL} \varepsilon_p^i h^i \quad [2.1]$$

where PD = pavement plastic (permanent) deformation

NSL = the number of sub-layers

ε_p^i = plastic strain in sub-layer i

h^i = thickness of sub-layer i

The design guide uses the constitutive relationship between prediction of rutting in the asphalt mixture and a field-calibrated statistical analysis of laboratory repeated load permanent deformation tests. The laboratory-derived relationship is then adjusted to match the rut depth measured from the roadway. A final form of the relationship can be expressed as (AASHTO 2008):

$$\Delta_{p(HMA)} = \varepsilon_{p(HMA)} h_{HMA} = \beta_{1r} k_z \varepsilon_{r(HMA)} 10^{k_{1r}} n^{k_{2r} \beta_{2r}} T^{k_{3r} \beta_{3r}} \quad [2.2]$$

where $\Delta_{p(HMA)}$ = accumulated permanent (or plastic) vertical deformation in the HMA layer/sublayer (in.)

$\varepsilon_{p(HMA)}$ = accumulated permanent axial strain in the HMA layer/sublayer (in./in.)

$\varepsilon_{r(HMA)}$ = resilient (or elastic) strain calculated by the structural response model at the mid-depth of each HMA sublayer (in./in.)

h_{HMA} = thickness of the HMA layer/sublayer (in.)

n = number of axle load repetitions

T = mix or pavement temperature (°F)

$$k_z = \text{depth confinement factor} = (C_1 + C_2 D) \cdot 0.328196^D$$

k_{1r}, k_{2r}, k_{3r} = global field calibration parameters; $k_{1r} = -3.35412$, $k_{2r} = 0.4791$, and

$$k_{3r} = 1.5606$$

$\beta_{1r}, \beta_{2r}, \beta_{3r}$ = local field calibration constants; for the global calibration these constants were all set to 1.0

$$C_1 = -0.1039(H_{HMA})^2 + 2.4868H_{HMA} - 17.342$$

$$C_2 = 0.0172(H_{HMA})^2 - 1.7331H_{HMA} + 27.428$$

D = depth below the surface (in.)

H_{HMA} = total HMA thickness (in.)

2.4 Finite Element Analysis for Flexible Pavements

The finite element technique is receiving increased attention from pavement mechanics because of its extremely versatile implementation of mechanical characteristics. These attributes address issues such as inelastic constitutive behavior, irregular pavement geometry (Helwany et al. 1998; Wang 2001; Blab and Harvey 2002; Erkens et al. 2002; Al-Qadi et al. 2002, 2004, 2005) and growing damage (Collop et al. 2003; Mun et al. 2004; Kim et al. 2006). As illustrated in figure 2.2, three different types of analysis models—axisymmetric, 2-D plane strain, and 3-D—are typically used by researchers to examine the performance of multilayered pavement structures.

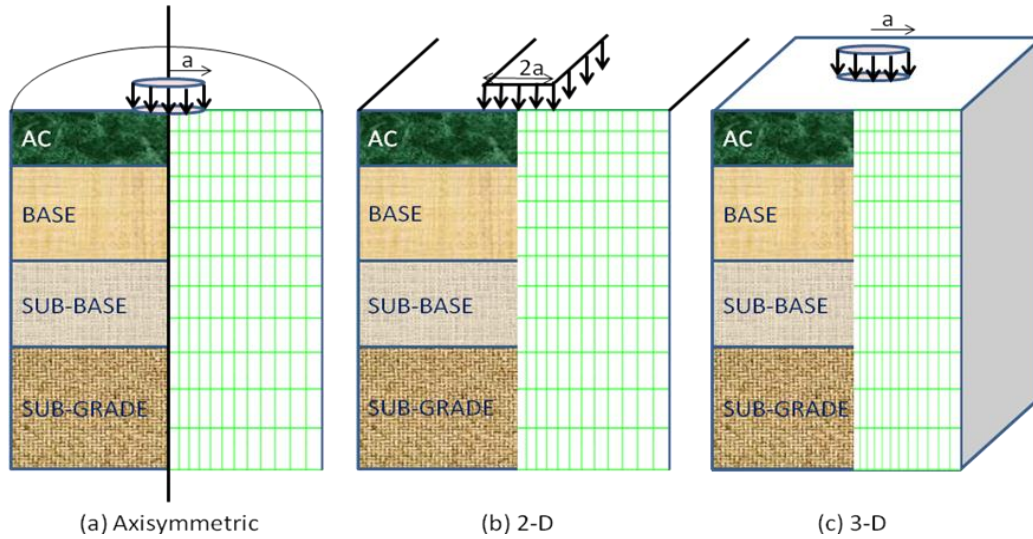


Fig. 2.2 Three Typical FE Analysis Models for Pavements

Each model presents pros and cons that are primarily dependent on modeling accuracy, simplicity, flexibility, and computational efforts. As a reference, the general aspects of each modeling approach are summarized in table 2.3.

Table 2.3 Summary of FE Modeling Approaches (Yoo 2007)

Condition	Axisymmetric	2-D Plane Strain	Three-dimensional
Loading	Static	Static	Static/Dynamic
Loading Area	Circular Single	Line Load	Versatile
Computation Time and Memory	Lowest	Middle	Highest Intensity
Interface Modeling	No	Partial	Yes
Discontinuity Modeling	No	Partial	Yes

2.4.1 Axisymmetric Approach

This model significantly reduces computational effort from 3-D pavement structures to 2-D cases by assuming constant material properties in all horizontal planes within cylindrical coordinate systems. As such, it has been widely used in pavement modeling despite its limitation in terms of loading configuration—it uses only circular single-tire loading.

Cho et al. (1996) investigated three different FE models, axisymmetric, 2-D plane strain and 3-D, to determine an appropriate model in terms of traffic loading effects on pavement responses. From linear elastic analysis, they found that axisymmetric and 3-D models yielded comparable results from typical layered elastic analyses, while the 2-D plane strain model overestimated responses.

The effects of loading configurations including axle type, axle load, and tire pressure at different vehicle speeds were investigated by Helwany et al. (1998) using FE analysis. It was reported, as can be expected, that the axle load significantly influenced pavement responses. An interesting finding from the study is that only the radial and the longitudinal strains were affected by tire pressure for the axisymmetric analysis and the 3-D analysis, respectively.

Myers et al. (2001) attempted 2-D plane strain analysis instead of the axisymmetric model by incorporating a correction factor, defined as the tensile stress ratio of axisymmetric analysis, to 2-D plane strain analysis. The results from 2-D plane strain with the correction factor were comparable to those from the axisymmetric model within the asphalt concrete surface layer.

2.4.2 Two Dimensional (2-D) Plane Strain Approach

The 2-D plane strain approach assumes that the longitudinal direction (traffic direction) of the pavement structure has no effect on pavement response due to the traffic loading. Therefore, the loading is applied as a strip load in the third dimension and an overestimation of load is induced.

Kim et al. (2005) investigated the effects of super-single (wide-base) tire loadings on pavements using 2-D plane strain and 3-D static or dynamic analyses. They examined the responses of pavement structure under two different sub-grade materials such as sand and clay. It was found that distresses from 2-D analysis were higher than those from 3-D analyses, and that the permanent strain induced by super-single tires was about four times greater than that of conventional tires.

Similarly, Soares et al. (2008) studied the effects of tire configurations by comparing pavement responses resulting from conventional dual tires with a wide-base single tire using the 2-D plane strain approach. In order to provide a more accurate estimation using the 2-D plane strain analysis, a factor showing the ratio between 3-D and 2-D was determined. Maximum displacements in the 2-D analyses were then divided by this factor to make a more realistic estimate. The pavement life was predicted by examining the permanent deformation of the surface layer subjected to each different tire configuration. It was concluded that the pavement life from conventional dual tires was longer than that from the wide-base single tire system.

2.4.3 Three dimensional (3-D) Approach

The three-dimensional (3-D) approach can simulate a pavement system more accurately and realistically than the aforementioned approaches. It is also capable of various conditions of analysis including dynamic loading, pavement discontinuities, and infinite and stiff foundation.

Elseifi et al. (2006) and Kim et al. (2008) conducted 3-D viscoelastic modeling for asphalt concrete layers to evaluate the asphaltic pavement structure by comparing distresses from the modeling with full-scale field test results. The results showed a good agreement.

The effects of loading conditions--such as tire imprint, non-uniform vertical pressure, un-equally distributed inflation pressure, and transverse loading--were investigated using the CAPA-3D FEM program (Perret 2002). Distresses were predicted and compared with results from conventional methods, but the latter did not account for the aforementioned loading conditions. The author concluded that transverse loading influenced pavement distresses in the most significant manner among all loading conditions considered.

Yoo (2007) performed 3-D finite element analysis to investigate damage which occurred in flexible pavements subjected to two different tire configurations: the dual tire assembly and the wide-base single tire assembly. In order to simulate moving wheel load more realistically, a continuous loading sequence was developed and applied instead of relying on a typical triangular or trapezoidal loading profile. Moreover, other factors including layer interface condition, tire footprint, and tangential shear force were taken into account. A better agreement with field performance data was produced by

considering the continuous loading sequence along with other factors rather than using the typical triangular or trapezoidal loading profile.

2.5 Material Models for Finite Element Analysis

As mentioned, the HMA surface layer is modeled as an isotropic viscoelastic medium. Constitutive behavior of the HMA layer can be represented by the following linear viscoelastic convolution integral:

$$\sigma_{ij}(x_k, t) = \int_0^t C_{ijkl}^{VE}(t - \tau) \frac{\partial \varepsilon_{kl}(x_k, \tau)}{\partial \tau} d\tau. \quad [2.3]$$

where $\sigma_{ij}(x_k, t)$ = stress as a function of time and space

$\varepsilon_{ij}(x_k, t)$ = strain as a function of time and space

C_{ijkl}^{VE} = stress relaxation modulus which is time-dependent

x_k = spatial coordinates

t = time of interest

τ = time-history integration variable

The constitutive equation is transformed into an incremental form in order to be used with a finite element technique. Briefly, this technique involves the use of numerical approximations that lead to a simple set of algebraic equations that are necessary to extract the finite element solution.

Isotropic viscoelastic materials can be modeled by a generalized Maxwell model, as shown in figure 2.3. This representation has proved to be so accurate that is

indistinguishable from the experimental data (Zocher et al. 1997). The mathematical formulation is represented by the following:

$$C_{ijkl}^{VE}(t) = C_{ijkl,\infty} + \sum_{p=1}^M C_{ijkl,p} \exp\left(-\frac{C_{ijkl,p}}{\eta_{ijkl,p}} t\right). \quad [2.4]$$

where $C_{ijkl,\infty}$ and $C_{ijkl,p}$ = spring constants in the generalized Maxwell model

$\eta_{ijkl,p}$ = dashpot constants in the generalized Maxwell model

M = the number of dashpots

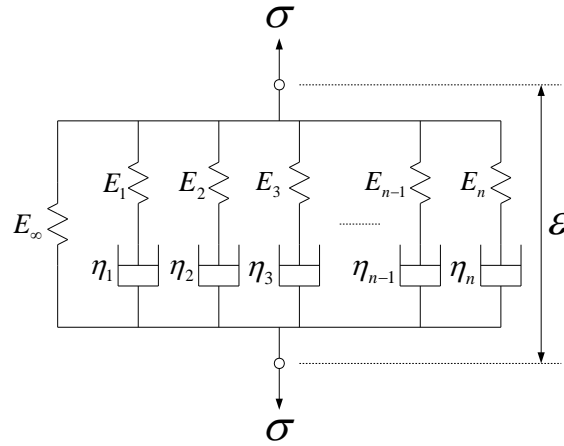


Fig. 2.3 Generalized Maxwell Model

Layers below the HMA surface layer are treated as linear elastic, similar to many other studies (Rowe et al. 1995; Papagiannakis et al. 1996; Siddharthan et al. 1998, 2002; Elseifi and Al-Qadi 2006). The linear elastic constitutive relationship can be expressed as:

$$\sigma_{ij}(x_k, t) = C_{ijkl}^E \epsilon_{kl}(x_k, t) \quad [2.5]$$

where C_{ijkl}^E = elastic modulus which is constant.

Chapter 3 MEPDG Analysis

Table 3.1 summarizes the key inputs used to perform the MEPDG analysis. As presented in the table, it was necessary to simplify or modify the MEPDG inputs to more strictly compare the results from the MEPDG simulations with those from the FEM analyses. Toward this end, only one type of vehicle, the Class 9 truck shown in figure 3.1, with no growth factor and transverse wander, was considered in this study. A total of 1,080 Class 9 trucks traveled through the design lane per day at a speed of 120 km/h, with a tire contact pressure of 830 kPa. Each truck passed in a uniform interval of 80 seconds.

Table 3.1 Summary of Traffic and Climate Inputs for MEPDG Analysis

Inputs	Details
Traffic	<ul style="list-style-type: none"> • AADT in the design lane per day: 1,080 • Operational Speed: 120 km/h
	<ul style="list-style-type: none"> • Vehicle Class Distribution: 100% of Class 9 • Hourly Distribution: uniform distribution • No Traffic Growth
	<ul style="list-style-type: none"> • Axle Load Distribution Factors: tandem axle (15,400 kg)
	<ul style="list-style-type: none"> • No Traffic Wander • Two Tandem Axles for Class 9 • Dual Tire Spacing: 30.48 mm • Tire Pressure: 830 kPa • Tandem Axle Spacing: 1,300 mm
Climate	<ul style="list-style-type: none"> • Lincoln, NE (modified to be constant temperature of 20° C)

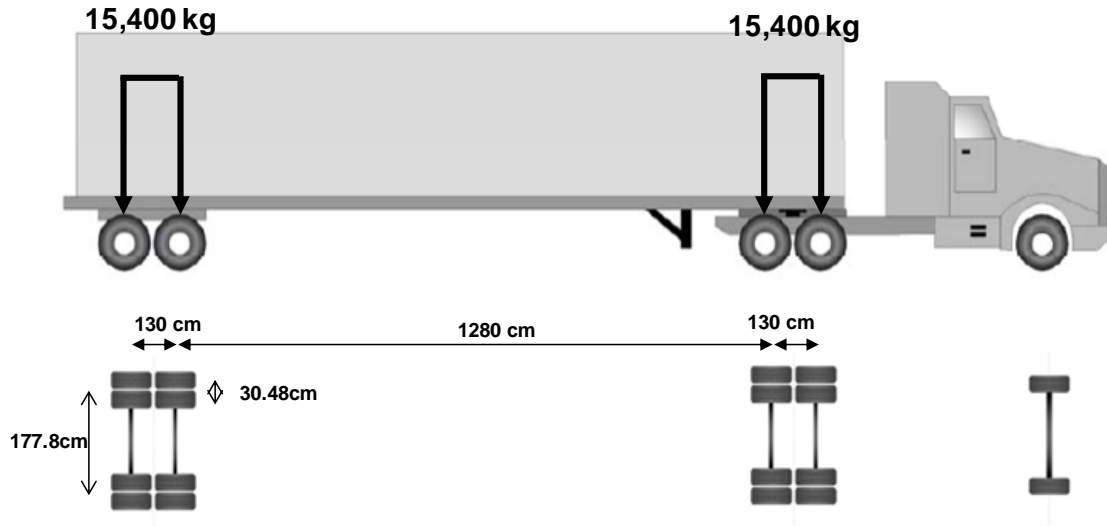


Fig. 3.1 A Typical Class 9 Truck

One of the advanced features of the MEPDG is the employment of the Enhanced Integrated Climatic Model, EICM, to consider climatic effects, such as temperature and moisture, during the whole pavement service life. This model allows the moduli of the layers to change over time and at different vehicle speeds. In an attempt to simplify the climate effect for a more explicit comparison between the two analysis methods, the pavement modeled herein is assumed to be under a constant temperature of 20°C with no moisture variation during the whole design life.

The mixture used for the asphalt layer was obtained from a field project located in Lincoln, Nebraska. The dynamic modulus test (AASHTO TP-62 2003) was performed to then identify the stiffness characteristics of the layer. From the dynamic modulus test, a value of 8,140 MPa was obtained for the elastic modulus of the asphalt layer. This is because the value 8,140 MPa was the stiffness at the truck speed of 120 km/h, which is equivalent to 9.5Hz loading frequency. Figure 3.2 shows the layer structure selected for this study and the material properties (modulus and Poisson's ratio) of each layer used to

perform the MEPDG analysis. The layer structure selected for this study is a typical four-layer system which consists of a 101.6-mm thick asphalt concrete layer, a 381-mm thick crushed-stone base, a 304.8-mm thick crushed gravel sub-base, and a semi-infinite A-6 type soil sub-grade. The elastic properties of the underlying layers (base, sub-base, and sub-grade) were assumed to have typical values for simplicity, while the viscoelastic properties of the asphalt layer were measured through the dynamic modulus test.

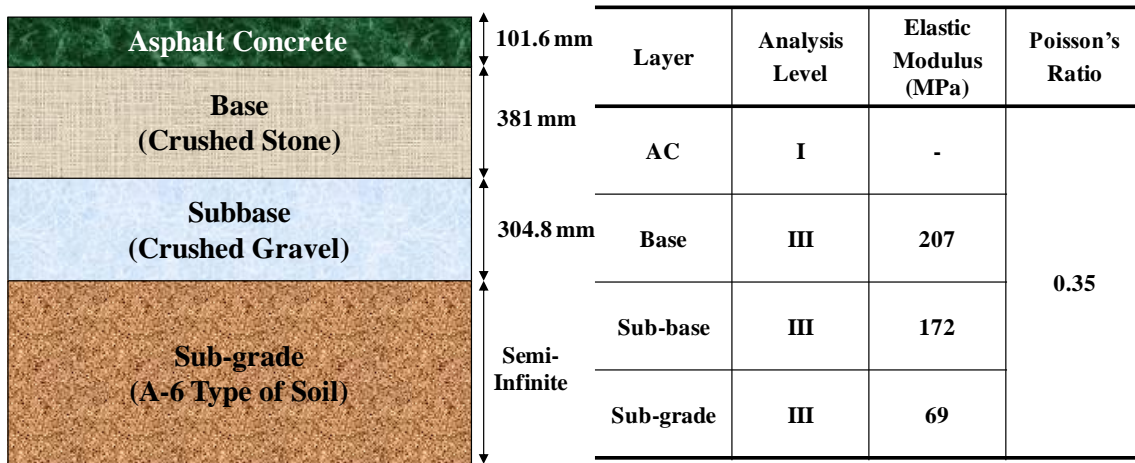


Fig. 3.2 Pavement Structure for this Study and Materials Properties for the MEPDG

Chapter 4 Finite Element Analysis

Parallel to the MEPDG analysis, a standard two-lane asphalt pavement was modeled through the FE method to investigate the mechanical performance behavior of the pavement resulting from Class 9 truck loading. The FE modeling was conducted by using a commercial FE package, ABAQUS Version 6.8 (2008). The model employed a time-marching computational simulation capable of predicting the spatial and temporal variations in stresses, strains, and displacements in the roadway. In reality, the design life of pavement is related to many different modes of energy dissipation, such as material viscoelasticity, cracking, and aging. However, as mentioned before, the current FE mechanistic modeling included only one source of energy dissipation — asphalt layer viscoelasticity — as a first step.

One of the distinct characteristics of finite element structural analysis is that the solution accuracy and computational costs are significantly dependent on the selected geometric features of modeling approaches (i.e., axisymmetric, 2-D plane strain, or 3-D), boundary conditions imposed, and size of the elements selected (mesh density). Therefore, to reach an appropriate pavement geometry that could be modeled and compared with the MEPDG analysis results, preliminary analyses investigating the effects of geometric features, boundary conditions, and mesh refinement were first conducted. Afterwards the appropriate pavement model, which is considered satisfactory in terms of both solution accuracy and computational efficiency, is found through the preliminary analyses. FE simulations are then conducted for the same pavement structure

employed to perform the MEPDG analysis. Layer materials and truck loading conditions are identical so that direct comparisons can be made between the two approaches.

4.1 Preliminary Analyses

Unlike the MEPDG analysis that assumes the semi-infinite dimension of pavement structure, domain size influences FE analysis results through its finite dimensions and corresponding boundary effects, or edge effect. An appropriate geometry for the modeling should not present any significant boundary effects. Accordingly, the FE model simulations are compared to the MEPDG results only to see the effect of surface layer material characteristics on the pavement's overall performance and life without incurring any geometric issues. To that end, four different sizes of FE domain were attempted, as illustrated in figure 4.1, and the displacement from the surface layer against varying sub-grade thicknesses was monitored. For this analysis, axisymmetric geometry was selected, and all materials of the pavement structure were assumed to be isotropic linear elastic. Fixed support at the bottom of the sub-grade layer was used, and horizontal displacements were constrained along the plane of symmetry (left side on the pavement). A circular load of 0.83 MPa with a contact area of 0.02 m² was applied to the pavement surface.

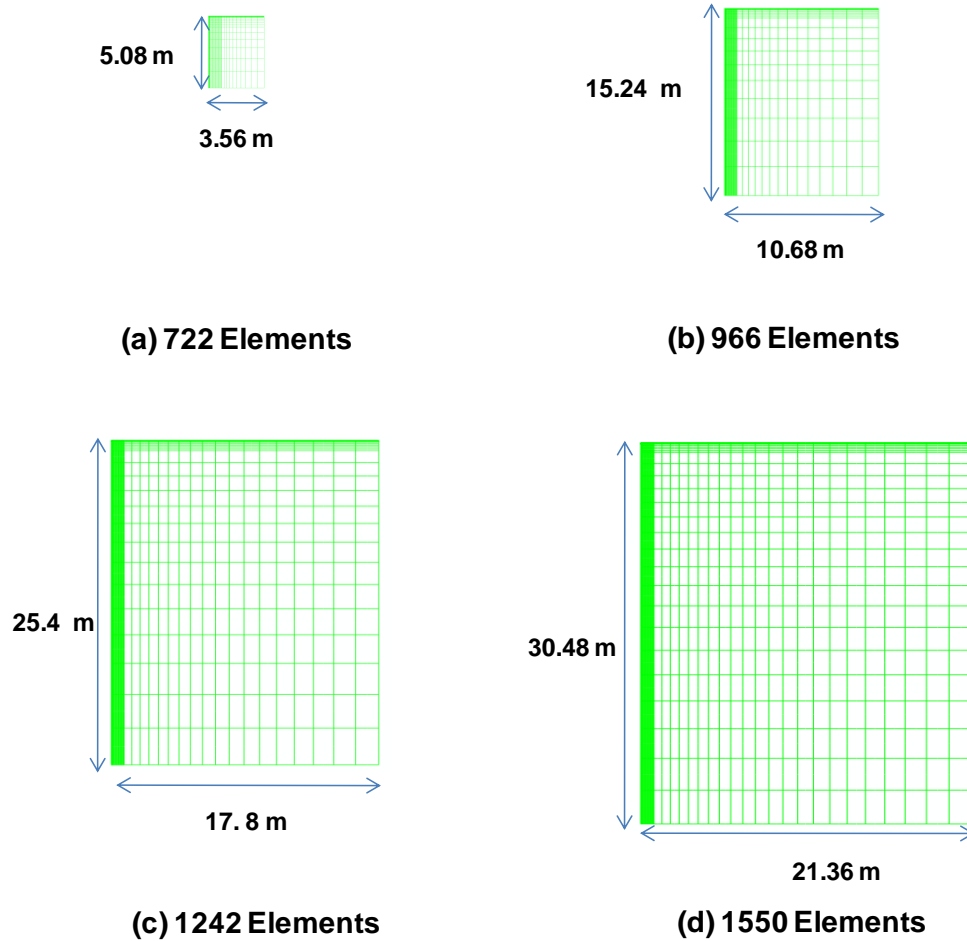


Fig. 4.1 Four Different Sizes of FE Domain Analyzed to Investigate End Effects

Analysis results clearly demonstrate the existence of boundary effects. As shown in figure 4.2, surface displacements converged as the thickness of the sub-grade layer increased. When the domain size is 25.4 m thick with a width of 17.8 m, the surface displacement stabilized and was not different from the case of 30.48 m thick.

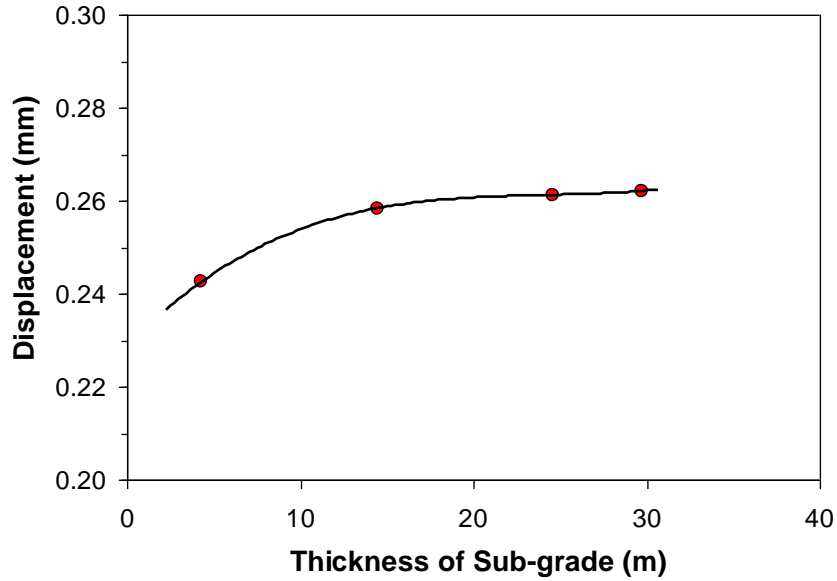


Fig. 4.2 Surface Displacements vs. Thickness of the Sub-grade Layer

With the converging domain size, 25.4 m thick with the width of 17.8 m, the effects of FE mesh refinements on pavement responses were then estimated. As is well known, fine meshes increase the computational costs, whereas choosing a relatively coarse mesh will result in an inaccurate numerical solution. Therefore, to reach an appropriate mesh density that produces satisfactory results, an analysis of mesh convergence is necessary. By re-creating the mesh with a denser element distribution, results from different meshes are compared.

The analysis was performed by increasing the element number in the loading area from 64 to 1,024 elements. Simulations results (displacements, strains, and stresses) on the top and at the bottom of the surface layer from each refinement were compared to results from a layered elastic analysis software, JULEA--the same analysis engine implemented in the MEPDG. Results are presented in table 4.1. As presented in the table, as the number of elements increases, FE simulation results converge and are closer to

JULEA results.

Table 4.1 FE Simulation Results with Different Number of Elements vs. JULEA Results

		JULEA	FEM (64 elements)	FEM (256 elements)	FEM (1,024 elements)	
DISPACEMENT (mm)	TOP	-0.267	-0.261	-0.261	-0.261	
	BOTTOM	-0.256	-0.250	-0.250	-0.250	
STRAIN	TOP	E11	-0.000217	-0.000196	-0.000205	-0.000209
		E22	0.000084	0.000062	0.000071	0.000076
		E33	-0.000217	-0.000196	-0.000205	-0.000209
	BOTTOM	E11	0.000226	0.000212	0.000219	0.000223
		E22	-0.000271	-0.000257	-0.000264	-0.000268
		E33	0.000226	0.000212	0.000219	0.000223
STRESS (MPa)	TOP	S11	-1.59	-1.49	-1.53	-1.56
		S22	-0.83	-0.83	-0.83	-0.83
		S33	-1.59	-1.49	-1.53	-1.56
	BOTTOM	S11	1.12	1.04	1.08	1.10
		S22	-0.15	-0.16	-0.15	-0.15
		S33	1.12	1.04	1.08	1.10

Based on the results presented in figure 4.2 and table 4.1, it is obvious that better accuracy in the FE pavement simulation can be reached by enlarging the analysis domain and refining mesh size. However, considering a huge number of load cycles over the whole service life of pavement structures, the enlarged domain size with extremely fine meshes for the simulation is clearly an obstacle for any practical purposes due to intensive computational costs. Therefore, any attempt to reduce the computational expense is pursued.

In an attempt to alleviate computational expense, infinite elements were used at the boundaries far from the loading zone, and significantly reduce the domain size of analysis: smaller domain size results in reduced computations. The infinite element is

generally applicable for the boundary value problems in which the region of interest is small in size compared to the surrounding medium. That is, standard finite elements are used to model the region of interest, while the infinite elements model the far-field region so as to reduce the domain size.

Figure 4.3 presents finite element meshes of axisymmetric, 2-D plane strain, and 3-D cases, respectively, with the infinite elements. As shown in the figure, the domain size using the infinite elements is 5.08 m thick and 3.56 m wide, and is much smaller than the domain size: 25.4 m thick with the width of 17.8 m. Due to the size reduction, computational costs can be dramatically saved as demonstrated in table 4.2, which records the time (in seconds) to finish a simulation of one loading cycle. Considering the significant load repetitions over the whole pavement life the use of infinite elements will clearly benefit simulation efforts.

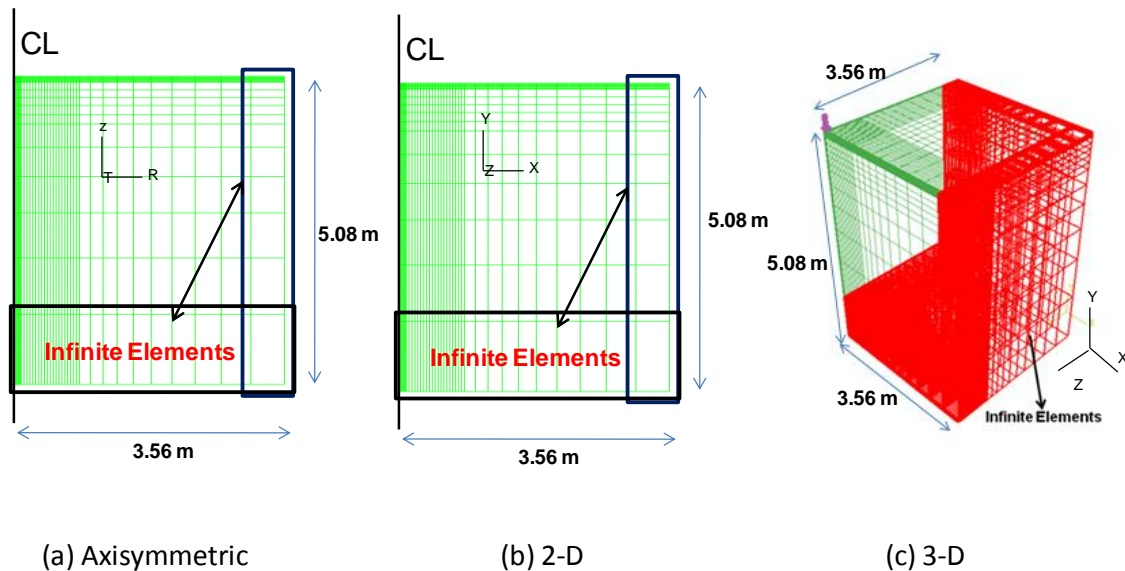


Fig. 4.3 Finite Element Meshes with Infinite Elements

Table 4.2 Comparison of Computation Costs of Each Model

		JULEA	Axisymmetric	2-D	3-D
Running Time (sec.)	Without Infinite Element	-	11	19	1,420
	With Infinite Element	-	10	9	882

The reduced computation benefit by using the infinite elements does not suffer modeling accuracy. As presented in table 4.3, FE analysis results between the two cases (with and without infinite elements) were very similar (or identical) between all three models (axisymmetric, 2-D plane strain, and 3-D). It should also be noted that the axisymmetric model is quite equivalent to the 3-D case and the layered elastic analysis by JULEA, whereas the 2-D plane strain presents much greater values than the other three approaches.

Tables 4.2 and 4.3 indicate that the axisymmetric modeling with infinite elements is attractive, since it is not computationally intensive and still produces equivalent results that are obtained from the realistic 3-D case. However, the axisymmetric modeling only allows a single circular loading on the pavement surface due to its rotational symmetry. It is limited to simulating real tire footprints that are not simply circular, and typical multiple-wheel loading configurations cannot be directly simulated.

Table 4.3 Summary of FE Simulations and Comparison with JULEA

Without Infinite Elements			JULEA	Axisymmetric	2-D	3-D
DISPACEMENT (mm)	TOP		-0.267	-0.261	-4.053	-0.249
	BOTTOM		-0.256	-0.250	-4.047	-0.237
STRAIN	TOP	E11	-0.000217	-0.000205	-0.000740	-0.000204
		E22	0.000084	0.000071	0.000249	0.000055
		E33	-0.000217	-0.000205	0.000000	-0.000176
	BOTTOM	E11	0.000226	0.000219	0.000531	0.000221
		E22	-0.000271	-0.000264	-0.000352	-0.000248
		E33	0.000226	0.000219	0.000000	0.000188
STRESS (MPa)	TOP	S11	-1.59	-1.53	-3.35	-1.49
		S22	-0.83	-0.83	-0.83	-0.83
		S33	-1.59	-1.53	-1.46	-1.42
	BOTTOM	S11	1.12	1.08	1.89	1.04
		S22	-0.15	-0.15	-0.36	-0.16
		S33	1.12	1.08	0.54	0.96
With Infinite Elements			JULEA	Axisymmetric	2-D	3-D
DISPACEMENT (mm)	TOP		-0.267	-0.260	-3.970	-0.238
	BOTTOM		-0.256	-0.249	-3.964	-0.227
STRAIN	TOP	E11	-0.000217	-0.000205	-0.000742	-0.000203
		E22	0.000084	0.000071	0.000251	0.000054
		E33	-0.000217	-0.000205	0.000000	-0.000175
	BOTTOM	E11	0.000226	0.000219	0.000536	0.000220
		E22	-0.000271	-0.000264	-0.000354	-0.000248
		E33	0.000226	0.000219	0.000000	0.000187
STRESS (MPa)	TOP	S11	-1.59	-1.53	-3.36	-1.48
		S22	-0.83	-0.83	-0.83	-0.83
		S33	-1.59	-1.53	-1.47	-1.41
	BOTTOM	S11	1.12	1.08	1.91	1.04
		S22	-0.15	-0.15	-0.36	-0.16
		S33	1.12	1.08	0.54	0.95

Even if axisymmetric modeling is not explicitly capable of addressing complex tire footprints, the multiple wheel loading configurations can be indirectly simulated. This is accomplished by using the superposition principle, that is, to simply superimpose responses monitored from different spots, or distances from the load center, induced by the single circular load for an equivalent response when multiple loads are involved. For example, suppose a typical single truck axle with dual tires, as shown in figure 4.4, is placed on the pavement. The displacement at the center of tire B is a superimposed displacement contributed by all four tires (A, B, C, and D) at different distances: 30.48 cm for tire A, 0 cm for B, 147.32 cm for tire C, and 177.8 cm for tire D.

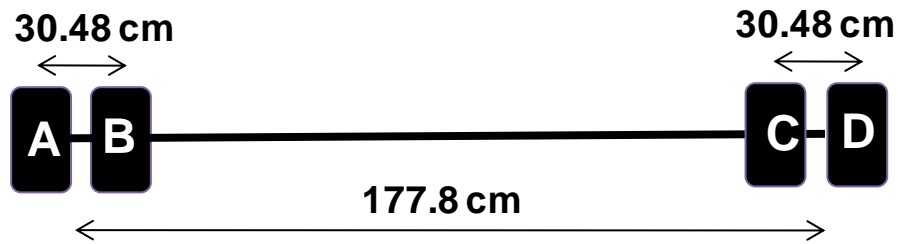
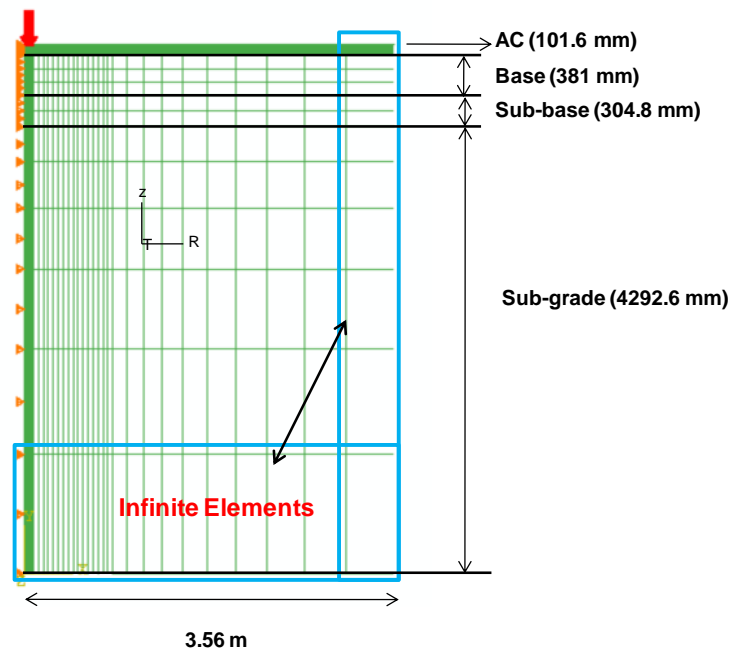


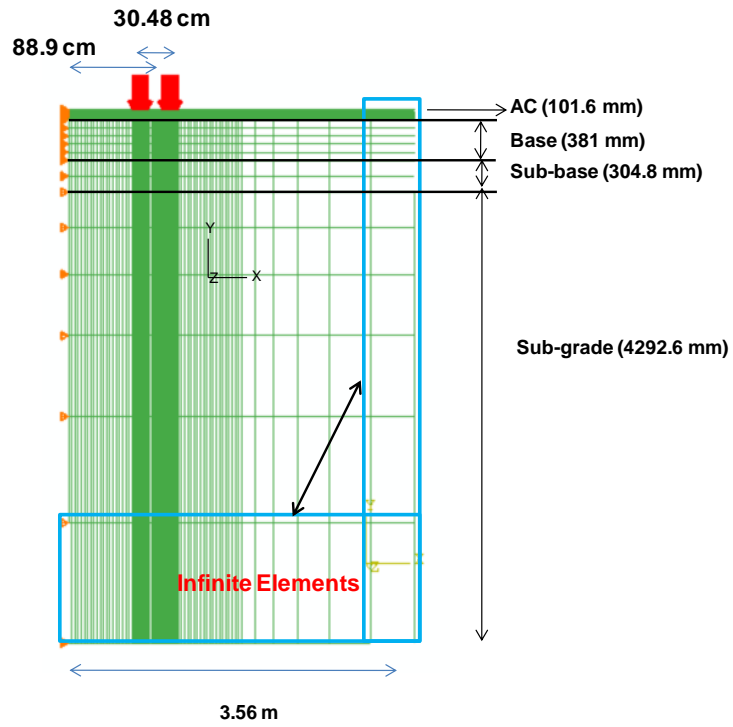
Fig. 4.4 A Typical Single Truck Axle with Dual Tires

Similar to the axisymmetric modeling, 2-D plane strain modeling is also advantageous over 3-D modeling since the computational time is considerably reduced. Nevertheless, as mentioned earlier with results from table 4.3, the 2-D plane strain condition assumes the infinite dimension in the third direction, or the traffic direction in the pavement structure. Therefore in this type of analysis the loading is applied as a strip load in the third dimension and an overestimation of load is induced.

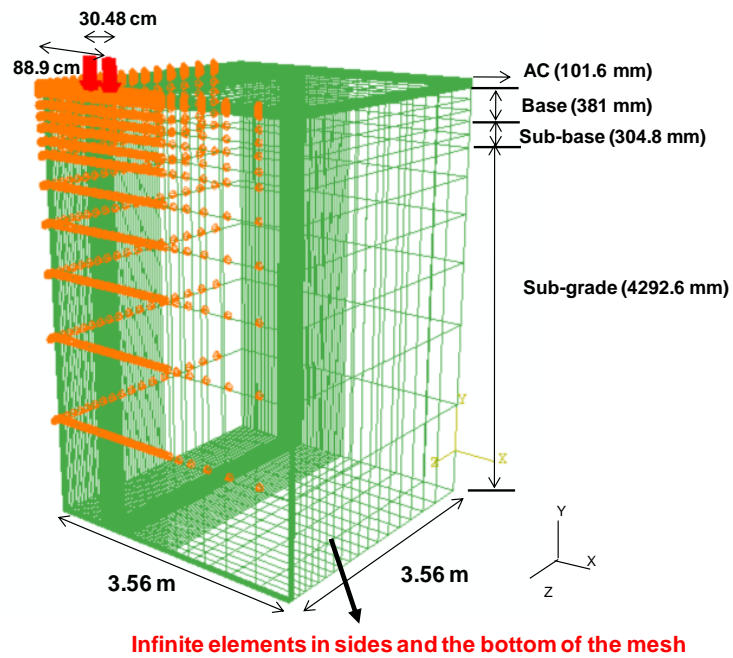
Figure 4.5 presents finite element meshes of each modeling approach. For the axisymmetric modeling, an 8-node bi-quadratic element with reduced integration (CAX8R in ABAQUS) for all pavement layers and a 4-node linear infinite element (CINAX4 in ABAQUS) for the far-field boundaries were adopted. The superposition was used to calculate pavement responses relative to dual circular tires. For the 2-D plane strain condition, a 4-node bilinear element (CPE4 in ABAQUS) for all pavement layers and a 4-node linear infinite element (CINPE4 in ABAQUS) along the far field boundaries were used with the dual tire configuration, as shown in the figure. In 3-D analysis, an 8-node linear brick with reduced integration (C3D8R in ABAQUS) for the standard finite element region and an 8-node linear infinite element (CIN3D8 in ABAQUS) for the bottom and horizontal far field boundaries were used. Two circular tires were placed on the pavement surface with axes of symmetry.



(a) Axisymmetric Model



(b) 2-D Plane Strain Model



(c) 3-D Model

Fig. 4.5 Finite Element Meshes and Boundary Conditions of Each Modeling

Table 4.4 summarizes pavement responses (i.e., displacement, stress, and strain) at various locations resulting from three different modeling approaches. As presented in the table, the axisymmetric approach with superposition is quite equivalent to the 3-D simulation, while the 2-D plane strain modeling yielded much higher values than those from the axisymmetric and the 3-D case.

In summary, each analysis exhibited pros and cons. Axisymmetric analysis was limited to account for realistic tire-axle configurations, but it can provide considerable savings in computational efforts. Furthermore, with the proper application of superposition, simulation results are quite equivalent to 3-D simulations. The 2-D plane strain modeling is very computationally efficient, but it generally produces overestimated responses that need calibrations for better accuracy. The 3-D simulation is the most accurate and versatile in applying any complex loading-axle-tire configurations, whereas it is computationally intensive. Considering modeling efficiency and accuracy together, the axisymmetric modeling approach incorporated with the infinite elements and the superposition principle seems to perform best. Consequently, the axisymmetric approach was selected to perform FE simulations of the pavement structure employed for the MEPDG analysis. Mechanical responses between the FE simulations and the MEPDG analyses are compared to monitor any significant differences. Pavement performance and design life between the two approaches are compared and discussed.

Table 4.4 Summary of Pavement Responses at Various Locations Resulting from Three Different Modeling Approaches

		A	A-B	B	C	C-D	D
Displacement (mm)	Axisymmetric	-0.478	-0.479	-0.492	-0.492	-0.479	-0.478
	2-D Plane Strain	-5.362	-5.588	-5.660	-5.660	-5.588	-5.362
	3-D	-0.388	-0.386	-0.402	-0.402	-0.386	-0.388
Strain (E11)	Axisymmetric	-0.00018	-0.00001	-0.00018	-0.00018	-0.00001	-0.00018
	2-D Plane Strain	-0.00062	-0.00044	-0.00062	-0.00062	-0.00044	-0.00062
	3-D	-0.00017	-0.00002	-0.00017	-0.00017	-0.00002	-0.00017
Strain (E22)	Axisymmetric	0.00009	0.00014	0.00009	0.00009	0.00014	0.00009
	2-D Plane Strain	0.00019	0.00024	0.00019	0.00019	0.00024	0.00019
	3-D	0.00006	0.00012	0.00006	0.00006	0.00012	0.00006
Strain (E33)	Axisymmetric	-0.00027	-0.00024	-0.00027	-0.00027	-0.00024	-0.00027
	2-D Plane Strain	0.00000	0.00000	0.00000	0.00000	0.00000	0.00000
	3-D	-0.00022	-0.00021	-0.00022	-0.00022	-0.00021	-0.00022
Stress (S11) (MPa)	Axisymmetric	-1.51	-0.37	-1.51	-1.51	-0.37	-1.51
	2-D Plane Strain	-2.90	-1.72	-2.89	-2.89	-1.72	-2.90
	3-D	-1.42	-0.36	-1.41	-1.41	-0.36	-1.42
Stress (S22) (MPa)	Axisymmetric	-0.83	0.03	-0.83	-0.83	0.03	-0.83
	2-D Plane Strain	-0.83	0.00	-0.83	-0.83	0.00	-0.83
	3-D	-0.83	0.00	-0.83	-0.83	0.00	-0.83
Stress (S33) (MPa)	Axisymmetric	-1.77	-0.95	-1.77	-1.77	-0.95	-1.77
	2-D Plane Strain	-1.30	-0.60	-1.30	-1.30	-0.60	-1.30
	3-D	-1.55	-0.84	-1.55	-1.55	-0.84	-1.55

4.2 Finite Element Modeling of the Pavement Structure

Figure 4.6 shows the axisymmetric dimension of the finite element mesh constructed for this study. As determined from the preliminary analyses, the geometry of the pavement is 5.08 m thick and 3.56 m wide, with infinite elements along the bottom and right side on the pavement (far-field) boundaries. Horizontal displacements were constrained along the plane of symmetry (left side on the pavement). A total of 256 elements were included in the loading zone.

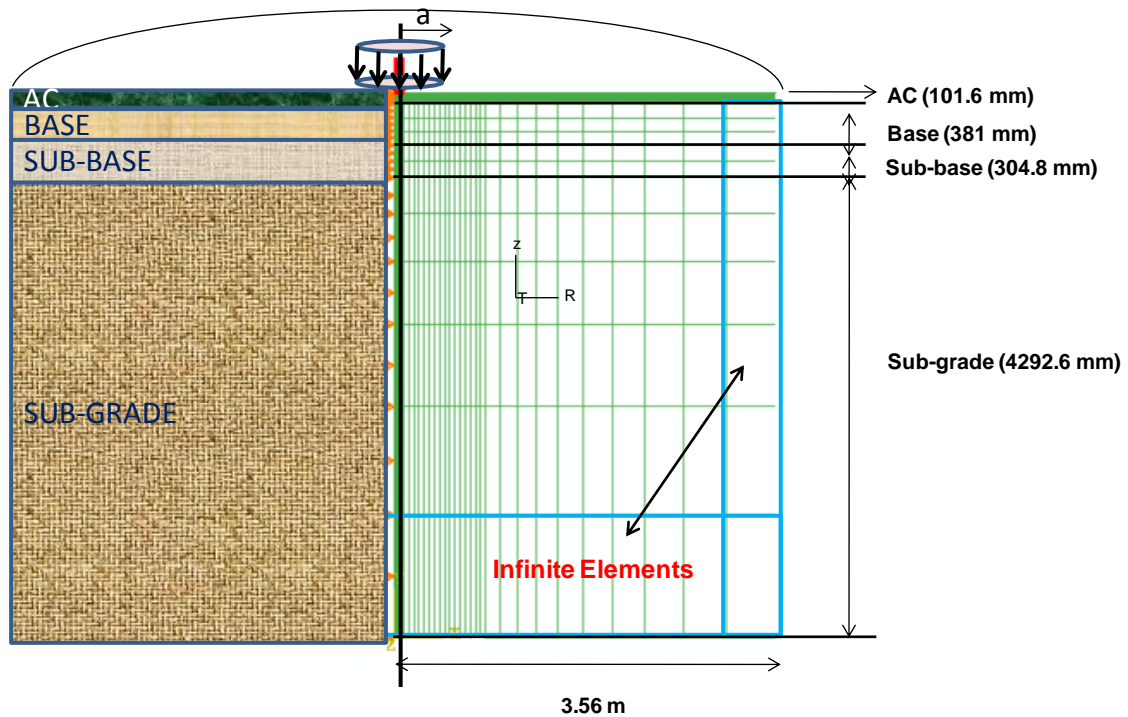


Fig. 4.6 Axisymmetric Dimension of the Finite Element Mesh for this Study

Figure 4.7 illustrates the loading configuration of the Class 9 truck used in this study (Soares 2005). As seen in this depiction, it consists of a front steer axle and two tandem axles with dual tires. In the analysis only the two tandem axles with dual tires were selected to reduce computational time. A 15.4-m Class 9 truck trailer traveling at 120 km/h takes 0.465 seconds to pass over a fixed point on the pavement. Therefore, the first truck passes the fixed point for 0.465 seconds and, after 80 seconds, a second truck passes through the same point. As shown in Figure 4.7, ramp functions with a peak load of 75 kN were used to represent the trailer axles and were implemented in the problem.

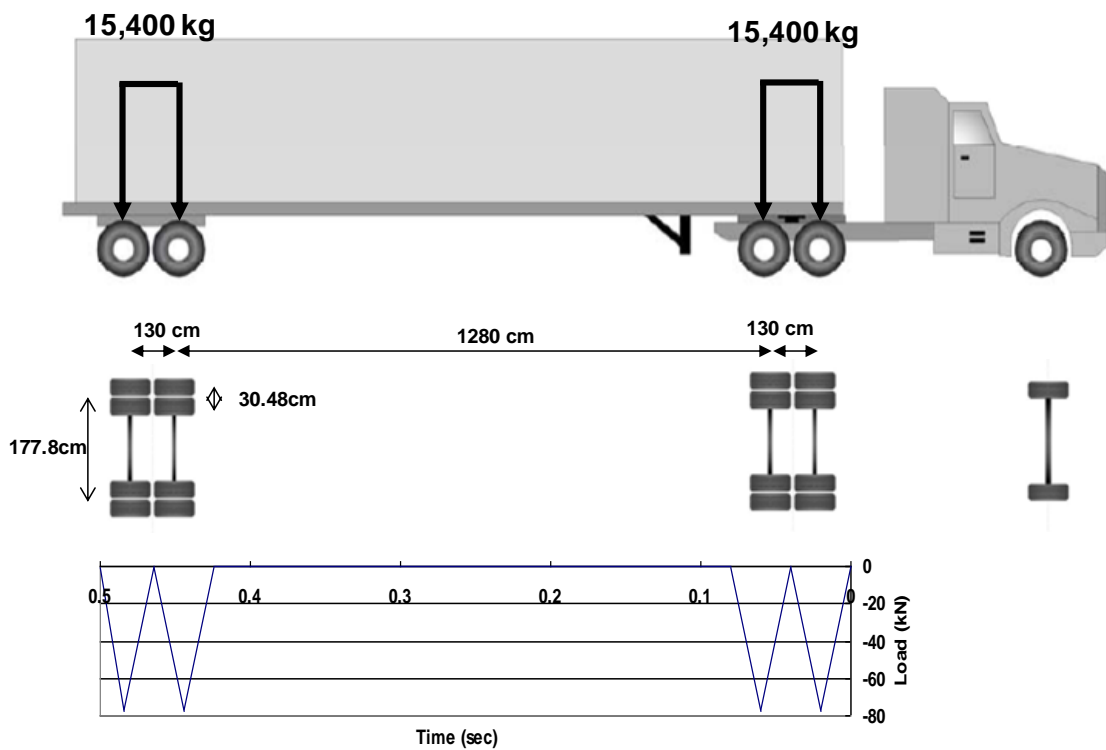


Fig. 4.7 Loading Configuration of the Class 9 Truck Used for the FE Modeling

To accomplish an equivalent analysis to the MEPDG, the underlying layers (i.e., base, sub-base, and sub-grade) were modeled as linear elastic. However, a linear viscoelastic response was considered to describe the behavior of the asphalt concrete surface layer. The asphalt layer can dissipate energy due to its viscoelastic nature, which results in permanent deformation (rutting) of the layer. As previously mentioned, the dynamic modulus test was performed to determine asphalt layer stiffness, and the results were used to define the linear viscoelastic material property of the asphalt concrete layer in a form of relaxation modulus, based on the generalized Maxwell model. Table 4.5 shows the mechanical material properties of each layer.

Table 4.5 Mechanical Material Properties of Each Layer for the FE Modeling

Elastic Material Properties		
	E (MPa)	ν
Base	207	0.35
Sub-base	172	
Sub-grade	69	
Viscoelastic Material Properties		
	Shear relaxation modulus (MPa)	Relaxation time (sec)
AC	10844.8	1.00E-05
	3229.3	1.00E-01
	2612.6	1.00E+00
	1723.6	1.00E+01
	971.3	1.00E+02
	488.7	1.00E+03
	51.5	∞

Chapter 5 Analysis Results and Discussion

The determination of failure criterion is necessary to define pavement life and to compare the performance of two methods (MEPDG and FEM). Since the FE modeling herein accounted for only one source of energy dissipation induced by the asphalt layer's viscoelasticity (which results in permanent deformation of the pavement surface layer), pavement life can only be estimated by examining rutting in the asphalt surface layer. A critical rut depth of 6.35 mm was used to determine pavement failure for this study, since it is a typical rutting performance criterion when only the surface layer is considered.

In the MEPDG analysis, the pavement life due to rutting is determined by using an empirically-developed performance prediction model (Equations [2.1] and [2.2] in Chapter 2) called the transfer function. The layered-elastic analysis in the MEPDG provides a vertical elastic strain in the asphalt layer, and the vertical elastic strain is used to calculate a permanent strain, as illustrated in the guide (NCHRP 1-37A 2004).

Finite element computer simulation requires a significant amount of computer processing and would make the determination practically unachievable, as it must be conducted over a long period of time until the pavement completely fails. Since life predictions in this study are not associated with damage but are simply based on viscoelastic permanent strain, it might be possible to extrapolate the results after a certain number of cycles have been simulated. This process was conducted by running the problem for up to 1,000 cycles, instead of for the full pavement life, and adding a trend line to the data for extrapolation. The data presented in figures 5.1 and 5.2 clarify this approach by illustrating permanent deformation on the surface layer.

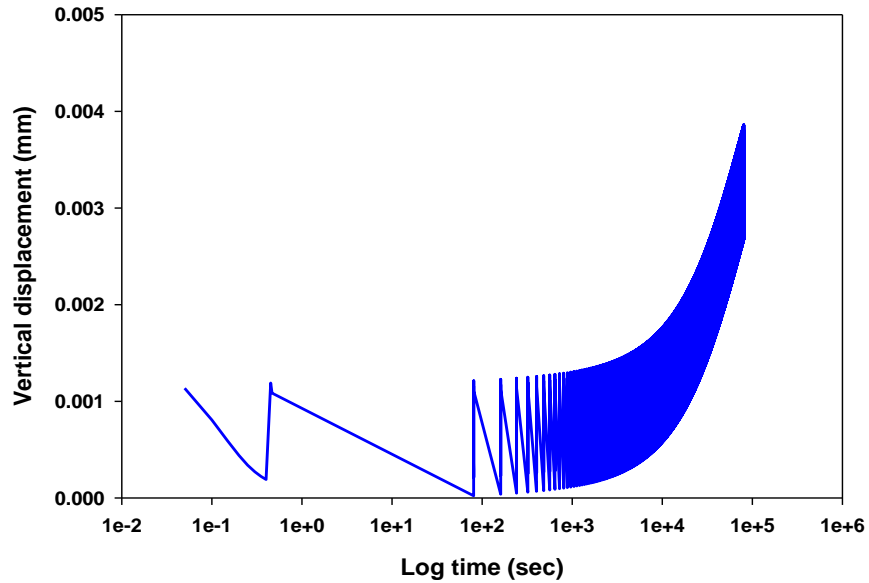


Fig. 5.1 Vertical Displacement vs. Time (from FEM)

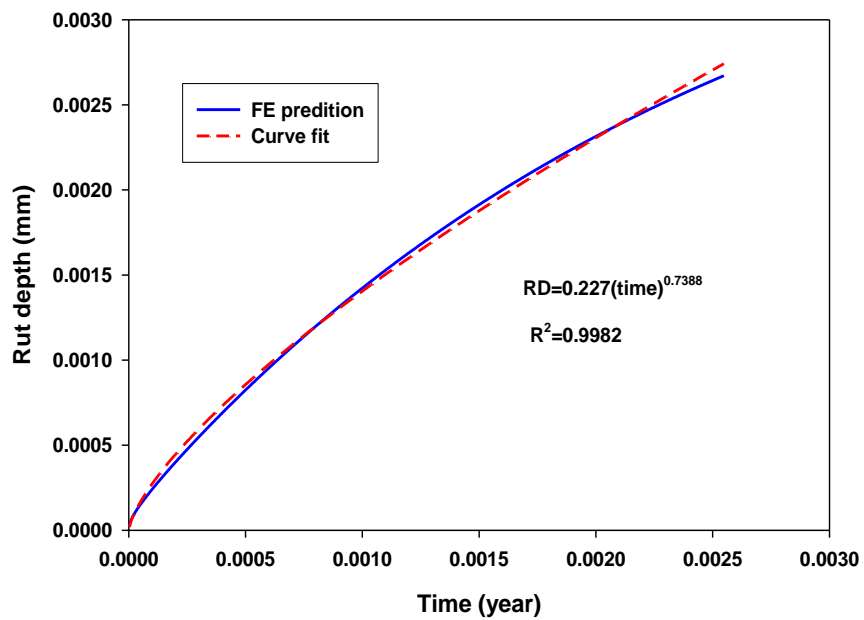


Fig. 5.2 Rut Depth vs. Time and Its Extrapolation (from FEM)

Figure 5.3 presents the analysis results (i.e., rut depth and pavement life at the critical rut depth of 6.35 mm) comparing the MEPDG and the FEM. As shown in the figure, the finite element mechanistic model produced a longer life than the MEPDG

approach. This is not surprising since the MEPDG accounts for pavement damage due to truck loading by incorporating pavement responses with the rutting transfer function that empirically characterize damage and failure. On the other hand, the finite element mechanistic model determines the pavement life by accounting for only one source of energy dissipation due to the viscoelastic asphalt layer.

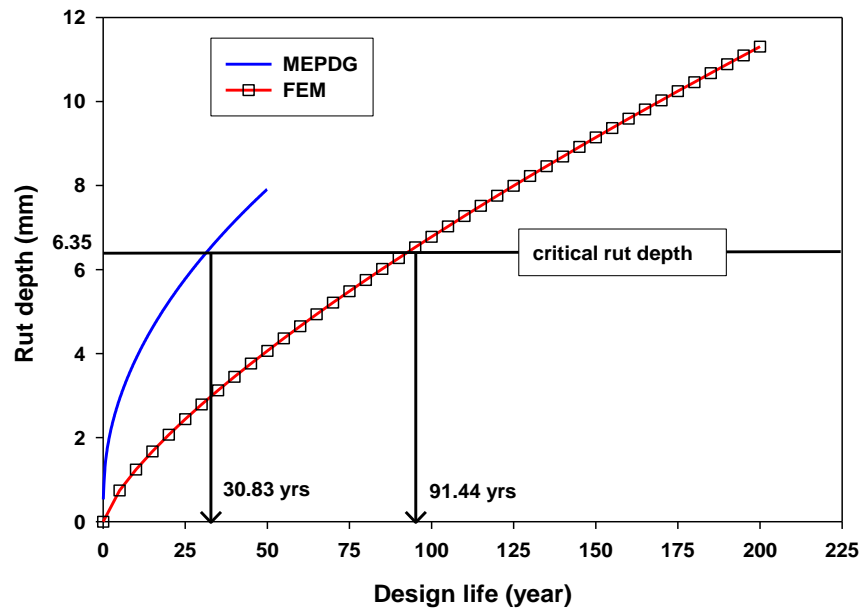


Fig. 5.3 Comparison of Pavement Performance and Life between MEPDG and FEM

The accuracy of pavement performance results from the mechanistic approach can be improved by considering other sources of energy dissipation in the model, such as cracking and aging. Then the life of the pavement will be shorter and closer to reality. One of the distinct characteristics of the mechanistic modeling approach is that it can reduce the empirical aspects of performance prediction models based on a more scientific rigor. Furthermore, the need for extensive laboratory and field work can be reduced, since the predictions rely upon computer simulation and the fundamental material properties of

individual layers. However, because the current generation of the FE model merely takes into account energy dissipation due to material viscoelasticity, and does not provide any sources of energy dissipation in the form of damage and due to environmental effects, it has limitations that are left to future work.

Chapter 6 Summary and Conclusions

The prediction for the performance and service life of pavement due to truck loads was made through the Mechanistic-Empirical Pavement Design Guide (MEPDG) and FE mechanistic analysis. For the MEPDG prediction, controlled and simplified inputs for the MEPDG analysis were used to more strictly compare the results from the MEPDG simulations with those from the FE analyses. Only one type of vehicle, the Class 9 truck traveling uniformly, was applied, and climate effects were not considered for the MEPDG analysis. The rut depth predicted by the performance prediction model was captured to compare with that of FE analysis.

For the FE analysis, three different models, axisymmetric, 2-D plane strain and 3-D, were explored to simulate pavement structures under multiple wheel loads. Among those—with all aspects such as modeling accuracy and efficiency related to the computational expense considered—for the FE simulations, we selected the axisymmetric model incorporated with infinite elements and the superposition principle for multiple wheel loads.

Analysis results indicated that the finite element mechanistic model produced a longer life than the MEPDG approach because the latter involved pavement damage through the empirical transfer function. The finite element mechanistic model, on the other hand, determined the pavement life by simply accounting for only one source of energy dissipation due to the viscoelastic asphalt layer. However, it is expected that the mechanistic approach for the prediction of pavement performance can be improved by

taking other sources of energy dissipation into account. These improvements remain a topic for future work.

References

- AASHTO. "Mechanistic-Empirical Pavement Design Guide." *A Manual of Practice*. Interim Ed. 2008.
- AASHTO TP-62. "Determining Dynamic Modulus of Hot-Mix Asphalt Concrete Mixtures." 2003.
- ABAQUS. Version 6.8. Pawtucket, RI: Hibbt, Karlsson, and Sorenson, Inc., 2008.
- Al-Qadi, I. L., A. Loulizi, I. Janajreh, and T.E. Freeman. "Pavement Response to Dual and New Wide Base Tires at the Same Tire Pressure." *Transportation Research Record*. 1806 (2002) : 38-47.
- Al-Qadi, I. L., M.A. Elseifi, and P.J. Yoo. "In-situ validation of mechanistic pavement finite element modeling." *Proc., 2nd Int. Conf. on Accelerated Pavement Testing*. Minneapolis, 2004.
- Al-Qadi, I. L., P.J. Yoo, and M.A. Elseifi. "Characterization of Pavement Damage Due to Different Tire Configurations." *Journal of the Association of Asphalt Paving Technologists*. 74 (2005) : 921-962.
- Blab, R., and J.T. Harvey. "Modeling Measured 3D Tire Contact Stresses in a Viscoelastic FE Pavement Model." *International Journal of Geomechanics*. 2.3 (2002): 271-290.
- Cho, Y. H., B. F. McCullough, and J. Weissmann. "Considerations on Finite-Element Method Application in Pavement Structural Analysis." *Transportation Research Record*. 1539 (1996): 96-101.
- Collop, A. C., A. Scarpas, Cor. Kasbergen, and A. Bondt. "Development and Finite Element Implementation of Stress-Dependent Elastoviscoplastic Constitutive Model with Damage for Asphalt." *Transportation Research Record*. 1832 (2003) : 96-104.
- Elseifi, M. A., and I.L. Al-Qadi. "Modeling of Strain Energy Absorbers for Rehabilitated Cracked Flexible Pavements." *Journal of Transportation Engineering*. 131.9 (2006): 653-661.
- Elseifi, M. A., I. L. Al-Qadi, and P. J. Yoo. "Viscoelastic Modeling and Field Validation of Flexible Pavements." *Journal of Engineering Mechanics*. ASCE. 132.2 (2006): 172-178.
- Helwany, S., J. Dyer, and J. Leidy. "Finite-Element Analyses of Flexible Pavements." *Journal of Transportation Engineering*. 124.5 (1998): 491-499.

- Kim, D., R. Salgado, and A. G. Altschaeffl. "Effects of Supersingle Tire Loadings on Pavements." *Journal of Transportation Engineering*. 131.10 (2005): 732-743.
- Kim, Y. -R., D. H. Allen, and G. D. Seidel. "Damage-Induced Modeling of Elastic-Viscoelastic Randomly Oriented Particulate Composites." *Journal of Engineering Materials and Technology*. 126 (2006) : 18-27.
- Kim, J., T. Byron, G. A. Sholar, and S. Kim. "Comparison of a Three-Dimensional Visco-Elastic Modeling and Field Validation of Flexible Pavements." TRB 2008 Annual Meeting. CD-ROM.
- Mun, S., M. Guddati, and Y.R. Kim. "Fatigue Cracking Mechanisms in Asphalt Pavements with Viscoelastic Continuum Damage Finite-Element Program." *Transportation Research Record*. 1896 (2004) : 96-106.
- Myers, L., R. Roque, and B. Birgisson. "Use of Two-Dimensional Finite Element Analysis to Represent Bending Response of Asphalt Pavement Structures." *International Journal of Pavement Engineering*. 2 (2001): 201-214.
- NCHRP 1-37A. "Guide for Mechanistic-Empirical Design of New and Rehabilitated Pavement Structures." Final Report. 2004.
- Papagiannakis, A. T., N. Amoah, and R. Taha. "Formulation for Viscoelastic Response of Pavements under Moving Dynamic Loads." *Journal of Transportation Engineering*. 122. 2 (1996): 140-145.
- Perret, J. "The Effect of Loading Conditions on Pavement Responses Calculated Using a Linear-Elastic Model." 3rd International Symposium. April 2-5. Amsterdam, 2002.
- Rowe, G. M., S.F. Brown, M.J. Sharrock, and M.G. Bouldin. "Viscoelastic Analysis of Hot Mix Asphalt Pavement Structures." *Transportation Research Record*. 1482 (1995): 44-51.
- Siddharthan, R. V., J. Yao, and P.E. Sebaaly. "Pavement Strain from Moving Dynamic 3D Load Distribution." *Journal of Transportation Engineering*. 124.6 (1998): 557-566.
- Siddharthan, R. V., N. Krishnamenon, M. El-Mously, and P.E. Sebaaly. "Investigation of Tire Contact Stress Distributions on Pavement Response." *Journal of Transportation Engineering*. 128.2 (2002): 136-144.
- Soares, R. F. "Finite Element Analysis of the Mechanistic of Viscoelastic Asphalt Pavements Subjected to Varying Tire Configurations." M.S. Thesis. Engineering Mechanics. U of Nebraska-Lincoln, 2005.

- Soares, R. F., D. H. Allen, Y. Kim, C. Berthelot, J. B. Soares, and M. E. Rentschler. "A Computational Model for Predicting the Effect of Tire Configuration on Asphaltic Pavement Life." *International Journal on Road Materials and Pavement Design*. 9.2 (2008): 271-289.
- Wang, J. "Three-dimensional Finite Element Analysis of Flexible Pavements." M.S. Thesis. U of Maine, 2001.
- Yoo, P. J. "Flexible Pavement Dynamic Responses Analysis and Validation for Various Tire Configurations." Ph.D. Dissertation. Civil Engineering. U of Illinois at Urbana-Champaign, 2007.
- Zocher, M. A., S.E. Groves, and D.H. Allen. "Three-Dimensional Finite Element Formulation for Thermoviscoelastic Orthotropic Media." *International Journal of Numerical Methods in Engineering*. 40.12 (1997): 2267-2288.